Structural Engineering and Mechanics, *Vol. 70, No. 1 (2019) 1-11*
DOI: https://doi.org/10.12989/sem.2019.70.1.001

Use of bivariate gamma function to reconstruct dynamic behavior of laminated composite plates containing embedded delamination under impact loads

Sang-Youl Lee[1a] and Jong-Su Jeon[*2]

[1]*Department of Civil Engineering, Andong National University, 1375 Gyeondong-ro, Andong, Gyeongsangbuk-do 36729, Republic of Korea*
[2]*Department of Civil and Environmental Engineering, Hanyang University, 222 Wangsimni-ro, Seongdong-gu, Seoul 04763, Republic of Korea*

(Received February 11, 2019, Revised February 22, 2019, Accepted February 24, 2019)

Abstract. This study deals with a method based on the modified bivariate gamma function for reconstructions of dynamic behavior of delaminated composite plates subjected to impact loads. The proposed bivariate gamma function is associated with micro-genetic algorithms, which is capable of solving inverse problems to determine the stiffness reduction associated with delamination. From computing the unknown parameters, it is possible for the entire dynamic response data to develop a prediction model of the dynamic response through a regression analysis based on the measurement data. The validity of the proposed method was verified by comparing with results employing a higher-order finite element model. Parametric results revealed that the proposed method can reconstruct dynamic responses and the stiffness reduction of delaminated composite plates can be investigated for different measurements and loading locations.

Keywords: bivariate gamma function; delaminated composite plates; micro-genetic algorithm; dynamic behavior; stiffness reduction

1. Introduction

Delamination in composite structures may lead to considerable stiffness reduction or change their dynamic behaviors. It is difficult to intuitively predict the dynamic behavior of composite structures containing delamination damage as a result of their complexity due to the combined effect of anisotropy and geometry in delamination. To alleviate the possibility of unexpected problems in service due to the delamination of composites, techniques that can predict the future behavior after the delamination occurs are needed.

Previous studies have used a guided or ultrasonic wave to detect on damage in composites. Williams *et al.* (2017) evaluated and imposed in-plane scattering matrices for the sparse array imaging of simulated damaged composites. Qi *et al.* (2009) used ultrasonic guided waves to develop a simulation toolbox for damage identification in composite structures. Luca *et al.* (2016) conducted a computational Lamb wave propagation in a laminated composite under impact loading. However, damage detection techniques based on sensitive waves may be infeasible in large-sized structures such as buildings or bridges. Such methods are complicated to be directly introduced to fiber-concrete hybrid structures because such sensitive waves are nonexistent in the real environments (Kim *et al.* 2012). To address these issues, other researchers have investigated these methods using time history data resulting from various impact loads. For example, Lee and Wooh (2005a) identified stiffness degradation in isotropic and composite plates on the basis of dynamic response data employing the micro-genetic algorithm (Micro-GA). Lee *et al.* (2007) accounted for stiffness reductions in laminated composite plates by conducting filtered noisy impact tests. Sharif-Khodaei *et al.* (2015) applied impact loads to identify damage in laminated composites using a self-diagnostic electro-mechanical impedance and neural networks. Chandrashekhar and Ganguli (2016) investigated the defect in laminated composites considering uncertainties of measurement and material based on free vibration data. However, the parametric examples which dealt with in the above researches are not of practical use since they considered a rectangular damage shape (Rus *et al.* 2006, Lee *et al.* 2008a, Trung *et al.* 2016). Rus *et al.* (2005) applied the boundary element method and typical genetic algorithms in order to determine in-plane damage in composites based on the first shear deformation theory (FSDT). This method has a limitation to predict damage shapes and loading conditions.

Lee *et al.* (2008b) suggested a modified bivariate Gaussian function to examine damage associated with cracks. It was observed that this approach can account for an elliptical defect configuration with a small number of unknown variables, and was implemented into concrete decks subjected to impact loading on the basis of the combination of finite element method (FEM) and the Micro-GA (Bhattacharya *et al.* 2016, Lee and Noh 2014). Park *et al.* (2009) employed the Gaussian function to detect defects in bridges, which imposed moving vehicles as input

∗Corresponding author, Assistant Professor
E-mail: jongsujeon@hanyang.ac.kr
[a]Associate Professor
E-mail: lsy@anu.ac.kr

 ISSN: 1225-4568 (Print), 1598-6217 (Online)

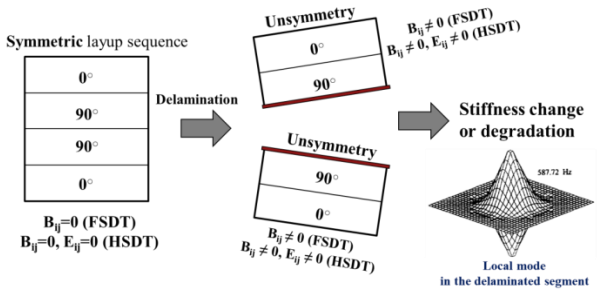

Fig. 1 Delamination effects on dynamic characteristics and mechanical properties

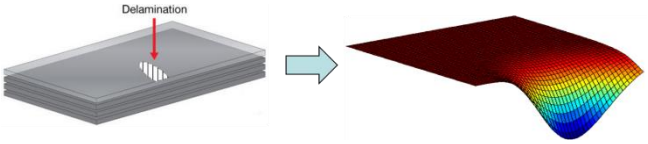

(a) Embedded delamination (b) Stiffness reduction shape

Fig. 2 Bivariate gamma function based representation of the stiffness reduction caused by delamination

loads (Noh and Lee 2013). Rus and Lee (2016) studied an optimal reconstruction of the damage distribution in bridge decks by measuring the noisy response induced by traffic loads. However, such studies can be applicable to only conventional structures made of concrete or steel materials. Moreover, existing methods based on the Gaussian function can only account for the symmetric damage shape.

This research proposes a mathematical method that can identify the stiffness degradation due to embedded delamination of composite plates under impact loads such as a seismic loading. Also, the combined method with the Micro-GA can reconstruct dynamic behavior after delamination associated with the combination of the identified stiffness reduction. To the best of this author's knowledge, on the basis of the bivariate gamma function, existing studies on the reconstruction of the dynamic behavior of delaminated composite structures are very scarce. Additionally, this study focuses on the dynamic response reconstruction of delaminated composites for different measurement, loading location, delamination locations, and fiber angles.

2. Gamma function based delamination model

In the two-dimensional FE delamination model, three element types at the boundary of a delamination exist; element without delamination and elements at the lower and upper delaminated regions (Noh and Lee 2014, Hua *et al.* 2002, Park and Lee 2009, Achache *et al.* 2017). It is noted that the delaminating layer is not symmetric, and thus its bending-twisting coupling stiffnesses are non- zero, as illustrated in Fig. 1. This physical characteristic yields various effects on the dynamic behavior of composites (Kassapoglou 2015).

The displacement field based on the FSDT can be written as

$$\begin{aligned} u^L(\zeta_1^L,\zeta_2^L,\zeta_3^L) &= u_0^L(\zeta_1^L,\zeta_2^L) + \zeta_3^L\phi_{\zeta_1}^L(\zeta_1^L,\zeta_2^L) \\ v^L(\zeta_1^L,\zeta_2^L,\zeta_3^L) &= v_0^L(\zeta_1^L,\zeta_2^L) + \zeta_3^L\phi_{\zeta_2}^L(\zeta_1^L,\zeta_2^L) \\ w^L(\zeta_1^L,\zeta_2^L,\zeta_3^L) &= w_0^L(\zeta_1^L,\zeta_2^L) \end{aligned} \quad (1)$$

where u_0^L, v_0^L and w_0^L are the components of the total displacement vector along the $(\zeta_1^L,\zeta_2^L,\zeta_3^L)$ coordinates. And, u_0^L, v_0^L and w_0^L are the translations along the coordinate lines of material point at the lower part in delamination, and $\phi_{\zeta_1}^L$ and $\phi_{\zeta_2}^L$ are the rotations in the $\zeta_2^L-\zeta_3^L$ and $\zeta_1^L-\zeta_3^L$ planes, respectively (Lee and Park 2009).

For a four-node element having five degrees of freedom (DOF) per node, a joint node is written as

$$\begin{aligned} \{\delta_\alpha^M\} &= \left[u_{0\alpha}^M \quad v_{0\alpha}^M \quad w_{0\alpha}^M \quad \phi_{\zeta_1\alpha}^M \quad \phi_{\zeta_2\alpha}^M\right]^T,\ \alpha=1,4 \\ \{\delta_\alpha^L\} &= \left[u_{0\alpha}^L \quad v_{0\alpha}^L \quad w_{0\alpha}^L \quad \phi_{\zeta_1\alpha}^L \quad \phi_{\zeta_2\alpha}^L\right]^T,\ \alpha=1,4 \end{aligned} \quad (2)$$

where δ_α^M and δ_α^L are the translations and rotations per node at the non-delamination and lower delamination parts, respectively. In this case, the eccentricity (e) of the neutral axes at the two parts is inevitable for the plate element (Ju *et al.* 1995). The discrepancy can be consistent with the continuity condition at the connecting boundary of the two parts.

$$w_{0\alpha}^M = w_{0\alpha}^L,\ \phi_{\zeta_1\alpha}^M = \phi_{\zeta_1\alpha}^L,\ \phi_{\zeta_2\alpha}^M = \phi_{\zeta_2\alpha}^L,\ \alpha=1,4 \quad (3)$$

By substituting Eq. (3) into Eq. (1), the DOF's relationship can be written as

$$u_{0\alpha}^L = u_{0\alpha}^M - e\phi_{\zeta_1\alpha}^M,\ v_{0\alpha}^L = v_{0\alpha}^M - e\phi_{\zeta_2\alpha}^M,\ \alpha=1,4 \quad (4)$$

Similarly, the following relationship can be obtained for the upper part of delamination.

$$\{\delta\}^{U\text{ or }L} = [T]\{\tilde{\delta}\}^{U\text{ or }L} \quad \{\tilde{\delta}\}^{U\text{ or }L} = \begin{bmatrix}\delta_1^M & \delta_2^{U\text{ or }L} & \delta_3^{U\text{ or }L} & \delta_4^M\end{bmatrix} \quad (5)$$

where the transformation matrix $[T]$ is used together with nodes. The element stiffness matrix $\left[\widetilde{K}\right]_e^{U\text{ or }L}$ and the mass matrix $\left[\widetilde{M}\right]_e^{U\text{ or }L}$ transformed by the matrix $[T]$ are written as

$$\begin{aligned} \left[\widetilde{K}\right]_e^{U\text{ or }L} &= [T]^T[K]_e^{U\text{ or }L}[T] \\ \left[\widetilde{M}\right]_e^{U\text{ or }L} &= [T]^T[M]_e^{U\text{ or }L}[T] \end{aligned} \quad (6)$$

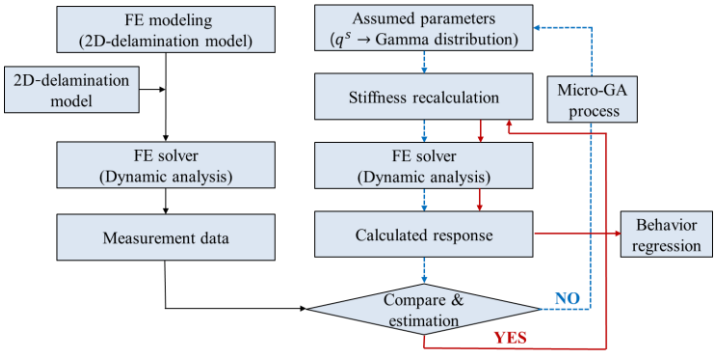

Fig. 3 An identification process of the location of a stiffness reduction owing to delamination and regression of response data

The distribution of the reduction in the stiffness associated with delamination can be obtained through the introduction of a modified bivariate gamma function with five unknown variables. The results for the bivariate chi-square distribution obtained by Gunst and Webster (1973) are extended to the bivariate gamma distribution function with unequal shape parameters $\gamma_1 < \gamma_2$ provided by Smith *et al.* (1982).

$$f(t_1,t_2;\gamma_1,\gamma_2,\eta) = \frac{t_1^{\gamma_1-1}t_2^{\gamma_2-1}\exp\left[-\frac{(t_1+t_2)}{1-\eta}\right]}{(1-\eta)^{\gamma_1}\Gamma(\gamma_1)\Gamma|\gamma_2-\gamma_1|} \times \sum_{k=0}^{\infty}\sum_{j=0}^{\infty}\frac{\eta^{j+k}}{(1-\eta)^{2j+k}}\frac{\Gamma(\gamma_2-\gamma_1+k)}{\Gamma(\gamma_2+j+k)}\frac{(t_1\cdot t_2)^j t_2^k}{j!k!},\ \eta = \rho^c\sqrt{\frac{\gamma_2}{\gamma_1}} \tag{7}$$

where $t_1 = \beta_1 x$, $t_2 = \beta_2 y$, β_1 is the scale factor of the x-coordinate of local damage, γ_1 the measure of dispersion along the x-axis, β_2 the scale factor of the y-coordinate of local damage, γ_2 the measure of dispersion along the y-axis, and ρ^c the correlation coefficient between the variables x and y. For the mth damaged element, Eq. (7) can be written as a single series formulation with regard to the modified Bessel function of the first kind ($I_v(z)$)

$$\begin{aligned} f(t_1,t_2;\gamma_1,\gamma_2,\eta) &= \frac{t_1^{\gamma_1-1}t_2^{\gamma_2-1}\exp\left[-\frac{(t_1+t_2)}{1-\eta}\right]}{(1-\eta)^{\gamma_1}\Gamma(\gamma_1)\Gamma|\gamma_2-\gamma_1|} \\ &\times \sum_{k=0}^{\infty}\frac{\eta^k\Gamma(\gamma_2-\gamma_1+k)t_2^k}{k!\,(\eta t_1\cdot t_2)^{k/2}}\cdot I_v(z) \\ &= \delta^{(m)} \end{aligned} \tag{8}$$

where

$$I_v(z) = z^v\sum_{j=0}^{\infty}\frac{(-1)^j z^{2j}}{2^{2j+v}j!\Gamma(v+j+1)},\ v = \gamma_1+k-1,\ z = \frac{2(\eta t_1\cdot t_2)^{1/2}}{1-\eta} \tag{9}$$

In the case of the stiffness reduction of a delaminated composite with dimensions of L_x and L_y in the x and y directions, the stiffness distribution at arbitrary x and y coordinates in the mth damaged element is written as

$$\lambda^{(m)}(\mathbf{x}) = 1-\delta^{(m)}(\mathbf{x}) \tag{10}$$

where $\lambda^{(m)}$ and $\delta^{(m)}$ refer to the stiffness reduction parameter and the degree of damage, respectively. The five unknown parameters in the gamma function are regarded as

$$\begin{aligned} \mathbf{p} &= [p^1 \quad p^2 \quad p^3 \quad p^4 \quad p^5]^T \\ &= [t_1 \quad t_2 \quad \gamma_1 \quad \gamma_2 \quad \eta]^T \end{aligned} \tag{11}$$

The variables t_1 and t_2 in Eq. (8) are transformed into the $(i\times j)$th element

$$t = \begin{Bmatrix} t_1 \\ t_2 \end{Bmatrix} = \begin{Bmatrix} \beta_1 x \\ \beta_2 y \end{Bmatrix} = \begin{Bmatrix} \beta_1\cdot i\cdot L_x/C_x^d \\ \beta_2\cdot j\cdot L_y/C_y^d \end{Bmatrix},\quad (i=1,2,\cdots,C_x^d \text{ and } j=1,2,\cdots,C_y^d) \tag{12}$$

where C_x^d and C_y^d are the number of divided elements in the x and y directions, respectively. The modified bivariate gamma function proposed here can account for delamination-induced stiffness degradation for an asymmetric shape in comparison to existing methods based on Gaussian functions, as illustrated in Fig. 2. In the Micro-GA, the stiffness reduction can be decided from the fluctuation in dynamic responses resulting from the delamination.

3. Stiffness identification and behavior reconstruction

The purpose of the proposed stiffness detection is to reconstruct dynamic behavior from the identification of the stiffness degradation associated with delamination damage. The accuracy of an existing gradient-based identification method may be impacted by insufficient initial input data. Because the overall procedure is related to the FE calculation in each iteration stage, the convergence is significantly dependent on the extent of the structural complexity. The Micro-GA has better convergence and accuracy in comparison to the conventional simple-GA (Mokaddem *et al.* 2014, Lee and Wooh 2005b). Thus, the Micro-GA is adopted in this study to solve the inverse problem, which reduces the computational efforts to compute the iterative FE process. In the inverse procedure, the FE model can describe the shift in the stiffness due to the delamination with five unknown parameters as indicated in Eq. (11). The following identification parameter vector in Eq. (11) is employed to estimate the local stiffness characteristics associated with the delamination.

$$\begin{aligned} \mathbf{p}^s &= [p^1 \quad p^2 \quad p^3 \quad p^4 \quad p^5]^T \\ &= [\beta_1 \quad \beta_2 \quad \gamma_1 \quad \gamma_2 \quad \eta]^T \end{aligned} \tag{13}$$

Table 1 Computational parameters for gamma function based micro genetic algorithms

Parameter	Range	Combinations	Binary digit	Population size	Maximum chromosome
β_1	1.5~10.0	8,192	15	5 (500~1,000 generations)	64
β_2	1.5~10.0	8,192	15		
γ_1	0.01~10.0	4,096	12		
γ_2	0.01~10.0	4,096	12		
η	0.01~0.95	1,024	10		

where β_1, γ_1, β_2, γ_2 are defined as before and η denotes the correlation factor between the parameters γ_1 and γ_2.

Dynamic response data obtained from combining the FEM and the Micro-GA are expressed as

$$Z(\mathbf{p}^s) = [{}^{11}U \quad {}^{12}U \quad \cdots \quad {}^{1N}U \quad \cdots \quad {}^{M1}U \quad {}^{M2}U \quad \cdots \quad {}^{MN}U] \tag{14}$$

where s is the number of identification variables, M the number of measurement locations, N the number of time steps, and ${}^{11}U$,…, ${}^{MN}U$ the dynamic response data. Thus, the detection of a stiffness reduction distribution yields a problem of computing identification variables in the gamma function when the values of the function Z match well with the measured data. Thus, the identification of a stiffness reduction distribution might be written as a minimization problem set as follows

$$\mathbf{MIN}\left(\Pi = \sum_{i=1}^{N}\left[{}^{i}\Psi - {}^{i}Z(\mathbf{p}^s)\right]^2\right) \tag{15}$$

where ${}^{1}\Psi$,…, ${}^{N}\Psi$ are the measured dynamic data computed in the forward procedure. Based on the combined FE analysis and GA, the overall distribution of the degraded stiffness associated with delamination can be obtained from the identification of the unknown variables $\mathbf{p}^s$.

Fig. 3 shows a procedure for detecting the location of damage associated with the delamination and regression of future responses employing the coupled gamma function and Micro-GA. From the combination of FE analysis and coupled Micro-GA based gamma function, the central location of a damaged region resulting from the delamination in composites, the overall distribution of the deteriorated stiffness, and the response predictions can be finally decided by identified unknown parameters, $\mathbf{p}^s$. From computing the unknown parameters, it is possible for the entire dynamic response data to develop a prediction model of the dynamic response through a regression analysis based on the measurement data. The reconstructed stiffness matrix at the *m*th element is written as

$$\tilde{\mathbf{K}}^{(m)} = \delta^{(m)}[\mathbf{K}]_e^m \tag{16}$$

At a divided time step, $t = (n+1)\Delta t$, the regressed displacement, $\tilde{\mathbf{u}}$, of the dynamic response data at each time step is expressed as

$$\tilde{\boldsymbol{u}}[n+1] = \left[\hat{\mathbf{K}} + \lambda_0\mathbf{M}\right]^{-1}\left[\hat{\mathbf{f}}[n+1] + \mathbf{M}(\lambda_0\mathbf{u}[n] + \lambda_2\dot{\mathbf{u}}[n] + \lambda_3\ddot{\mathbf{u}}[n])\right] \tag{17}$$

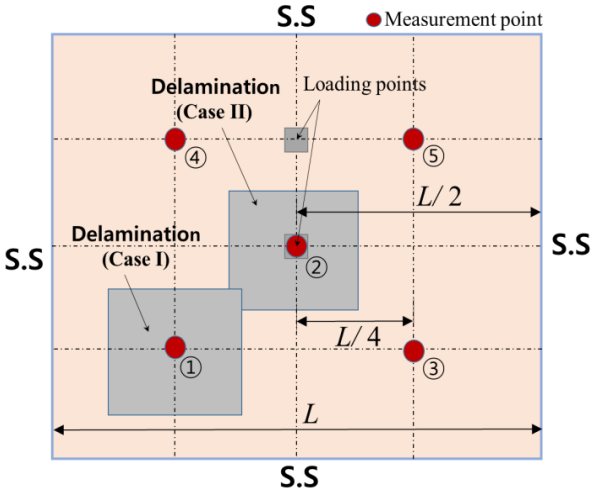

Fig. 4 Numerical model for parametric examples

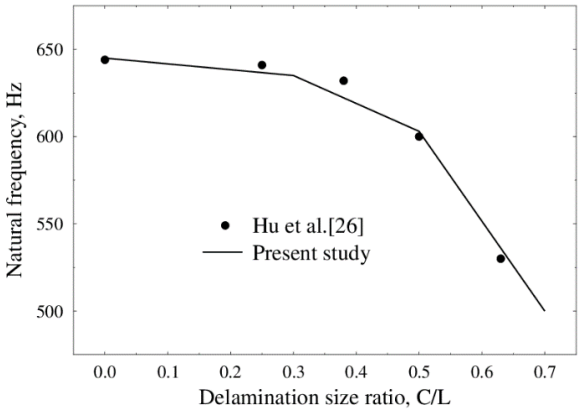

Fig. 5 Comparison of first natural frequencies for increase delamination sizes

where $\hat{\mathbf{f}}$ indicates the effective load at the next time step, $\hat{\mathbf{K}}$ is the reconstructed system stiffness matrix, $\dot{\mathbf{u}}$ is the velocity vector, $\ddot{\mathbf{u}}$ is the acceleration vector, and λ_0, λ_2, and λ_3 are constants for the time integration in Newmark's method.

4. Numerical examples

4.1 Numerical model and verification

[0/90]s and [45/-45]s laminates under impact loads are

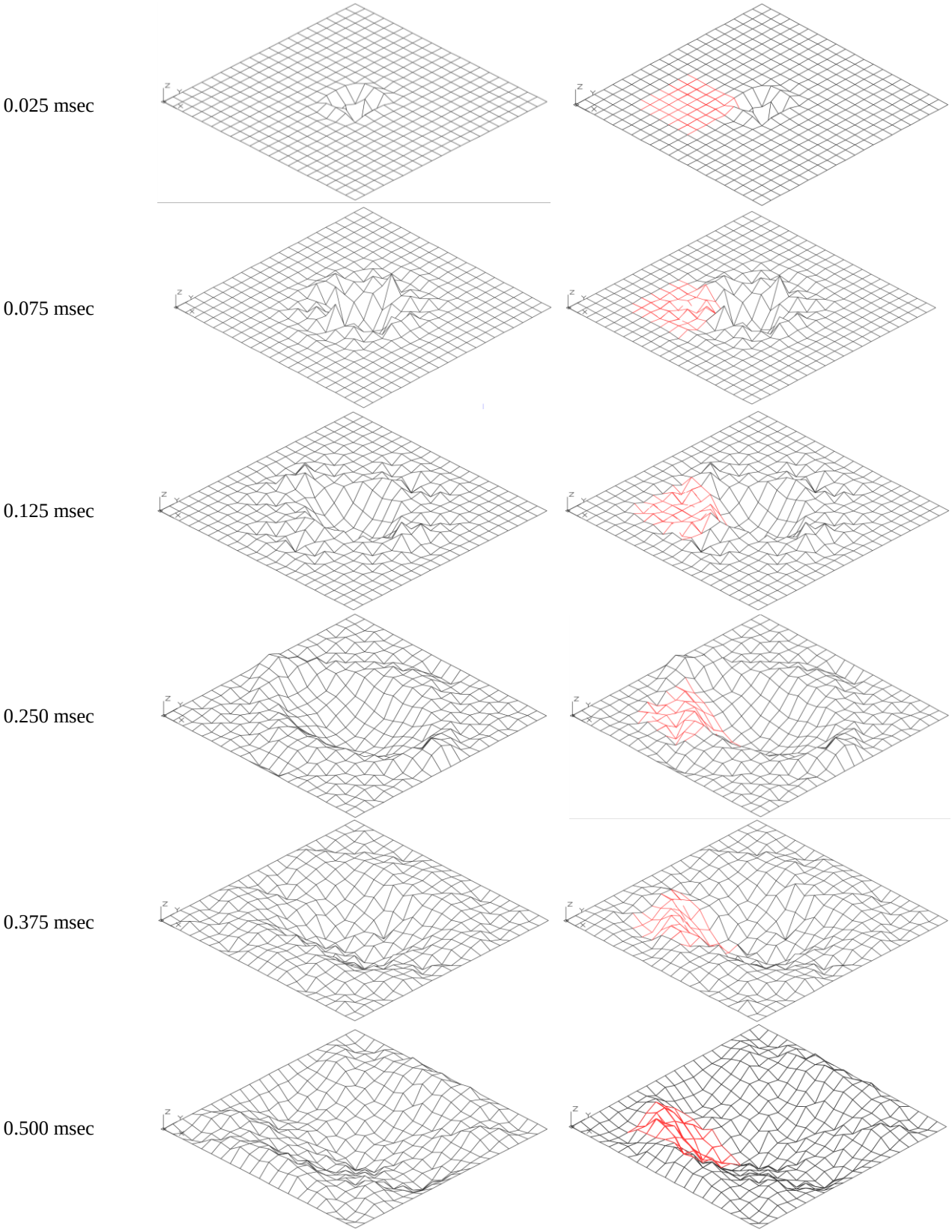

(a) Without delamination (b) With delamination

Fig. 6 Comparison of overall dynamic behaviors of composites without and with delamination. (Case II, *a*/*h* = 100, [0/90]s)

considered for the numerical example. For convenience, this study assumes the load $F(t)$ as a narrow rectangular pulse of width t_0

$$F(t) = F_0[H(t) - H(t - t_0)] \tag{18}$$

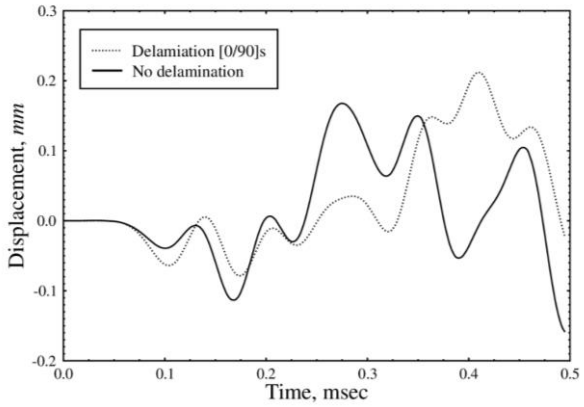

(a) Measurement 1

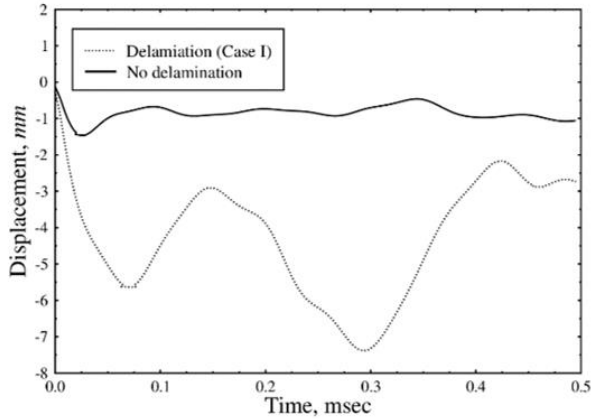

(b) Measurement 2

Fig. 7 Dynamic responses of composites with and without delamination at measurement locations (Case I, a/h = 100, [0/90]s)

where $H(t)$ is the Heaviside step function and F_0 is the magnitude of the load. This approximation is believed to be reasonable for impact loadings. Its pulse magnitude and duration are 100 kg and 50 μsec, respectively. The time step (Δt) used in the computation is 10 μsec. The geometry and material properties are as follow: $L = 1.0$ m, $a/h = 100$, $E_1 = 52.5$ GPa, $E_1/E_2 = 25$, $G_{12} = G_{13} = G_{23} = 10.5$ GPa, $\nu_{12} = 0.25$, and $\rho = 800$ kg/m^3.

Fig. 4 shows different delamination locations, loading points, and monitoring (measurement) points used in in the numerical model of simply supported composite plates. A concentrated step loading with a magnitude of 100 kN is applied at the upper or center of the plate. Table 1 indicates the computational parameters for damage detection associated the Micro-GA. In the inverse procedure, the location and degree of stiffness degradation owing to delamination are determined, and the reconstruction of the entire time history data is then computed.

To validate the two-dimensional delamination model applied in this research, the induced natural frequencies are compared with those in the literature. Fig. 5 compares first natural frequencies of all clamped composites for increased delamination sizes. In the figure, C and L are the delamination size and the length of a plate, respectively. The applied plate model is developed on the basis of the

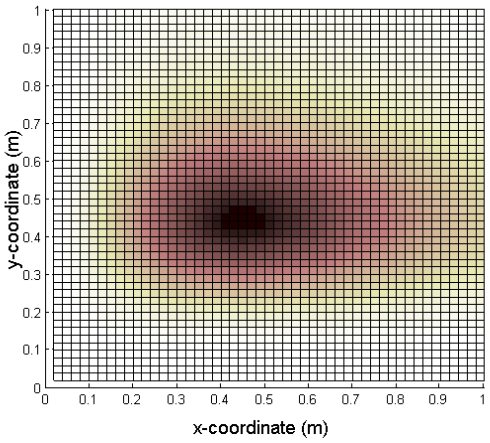

(a) x-y plane view

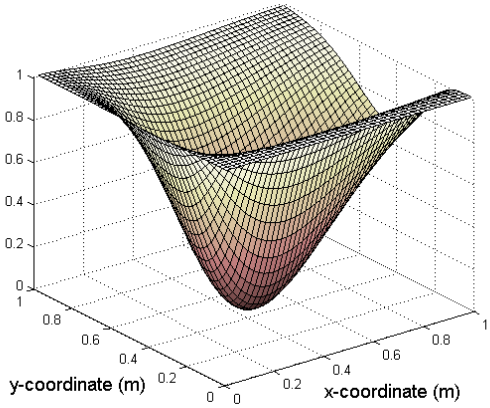

(b) 3D view

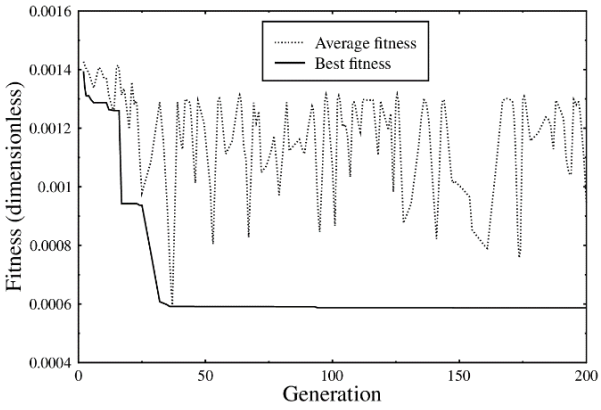

(c) Micro-GA process

Fig. 8 Determination of gamma function based delamination location, stiffness reduction, and Micro-GA procedure (upper loading, Case I, [45/-45]s)

higher-order shear deformation theory. Dimensions of the plate of eight plies $[0/90]_{2s}$ are 127 × 127 × 1.016 mm^3. A square embedded delamination is located at the center of the plate and on the mid-plane of the plate in the thickness direction. Material constants of a lamina (T300/943) are: $E_1 = 134$ GPa, $E_2 = 10.3$ GPa $G_{12} = G_{13} = 5.00$ GPa, $G_{23} = 3.28$ GPa, $\nu_{12} = 0.33$, and $\rho = 1{,}480$ kg/m^3. Note that these properties are used for only this example. It is found from the figure that the results for different delamination sizes obtained from this study match well with those of Hu *et al.* (2002).

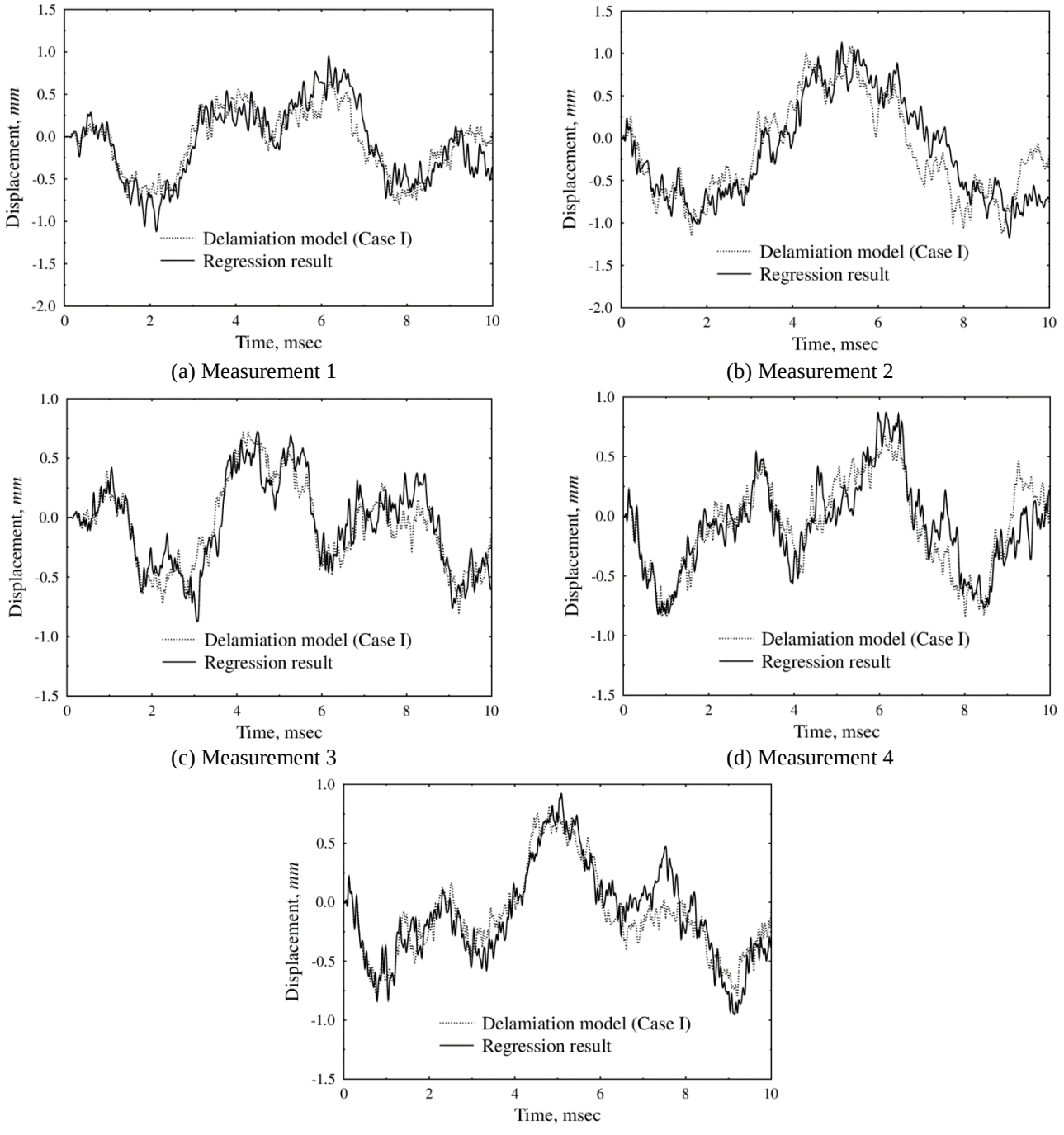

(a) Measurement 1

(b) Measurement 2

(c) Measurement 3

(d) Measurement 4

(e) Measurement 5

Fig. 9 Reconstructions of time history data of laminated composites with [45/-45]s for different measurement locations (upper loading, Case I)

Fig. 6 presents the difference between the overall dynamic behavior of the [0/90]s laminates for the delamination existence. It is indicated that the difference between the two behaviors increases as the time increases as a result of the delamination effects, especially for the delamination region. Fig. 7 shows comparisons of the dynamic response with and without delamination at various measurement locations. It is observed that the dynamic behavior of the two plates is similar at the region without delamination.

4.2 Stiffness detection and behavior reconstruction

The proposed algorithm regarding the modified bivariate gamma function was used to detect the stiffness distribution in composite plates. Fig. 8 shows the delamination identification in [45/-45]s laminates subjected to upper loading. Fig. 8(a) represents the calculated location and the extent of stiffness reduction owing to the delamination. Fig. 8(b) presents a three-dimensional view of the estimated stiffness degradation. Fig. 8(c) shows the best and average fitness values in the Micro-GA, as well as the mean of the best value of the population in each generation. In the figure, the best fitness value

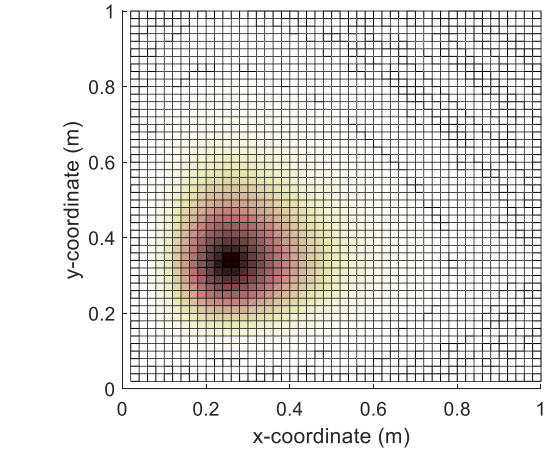

(a) x-y plane view

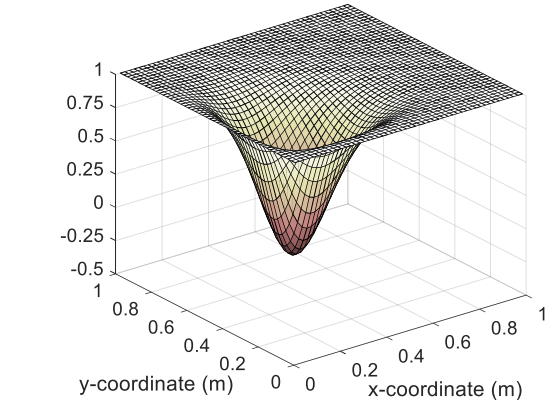

(b) 3D view

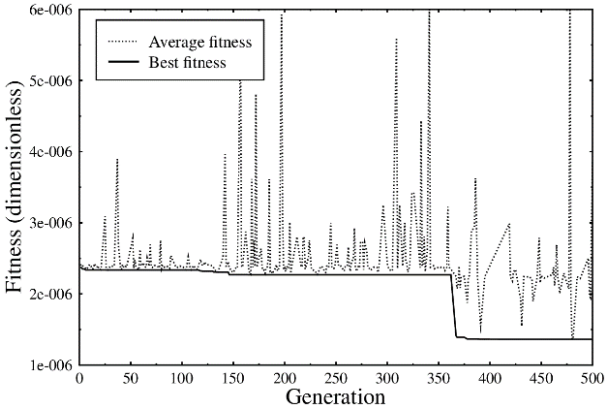

(c) Micro-GA process

Fig. 10 Determination of gamma function based delamination location, stiffness reduction, and Micro-GA procedure (central loading, Case II, [45/-45]s)

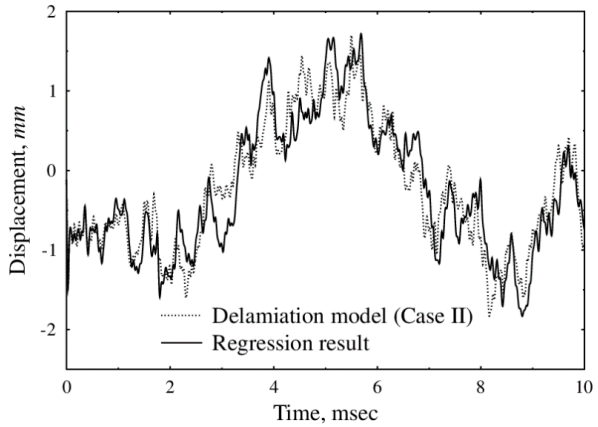

(a) Measurement 2

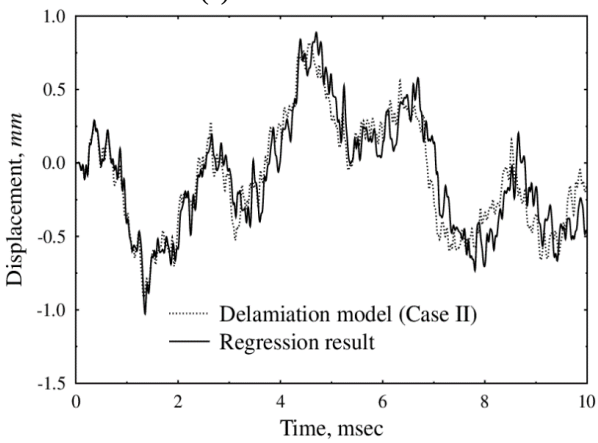

(b) Measurement 3

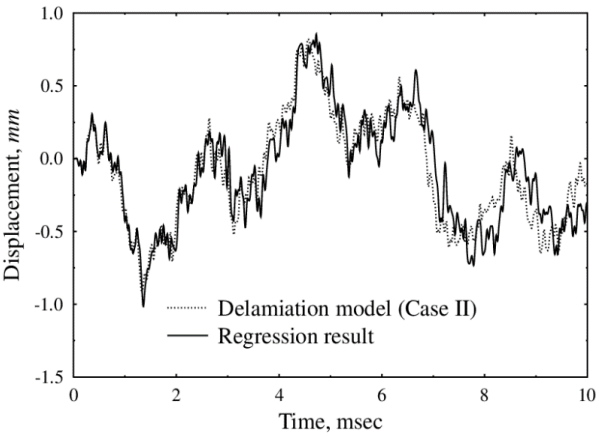

(c) Measurement 4

Fig. 11 Reconstructions of time history data of composites with [45/-45]s for different measurement locations (central loading, Case II)

asymptotically decreases to the zero residual value. Figs. 9(a) through (e) show comparisons of the measured and reconstructed time history data in laminates for different measurement locations. As observed, the regressed displacements are similar with the true ones in global behaviors.

Fig. 10 presents results of Case II under the same conditions as those in Case I, except for central loading. It can be found from the figure that the detection in Case II also seems to be accurate, as identified in Case I. Use of the bivariate gamma function highlighted that the proposed method approaches to the true values. On the other hand, the convergence rate varies from case to case, as shown in Fig. 10(c). The extent of stiffness reduction is dependent on the location of the delamination and loading condition. Figs. 11(a) through (c) show comparisons of the true and reconstructed time history data in composites for measurements 2-4.

As may be observed from the figures, the entire regressed time history data are slightly different from the measured ones. This difference is not significant because

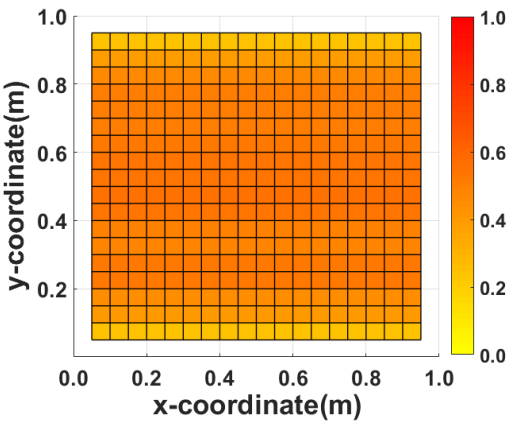

(a) [0/90/90/0]

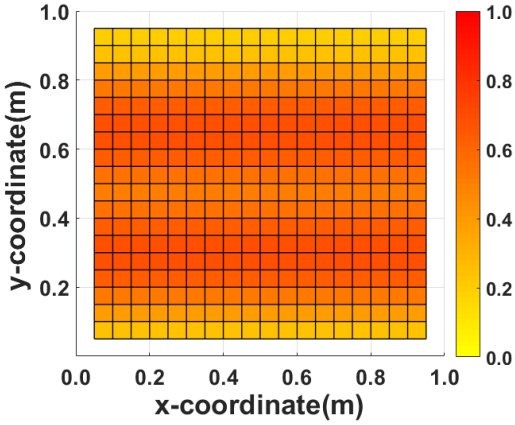

(b) [45/-45/-45/45]

Fig. 12 Induced correlation coefficients of the reconstruction of dynamic responses of composites for all measurement locations (upper loading, Case I)

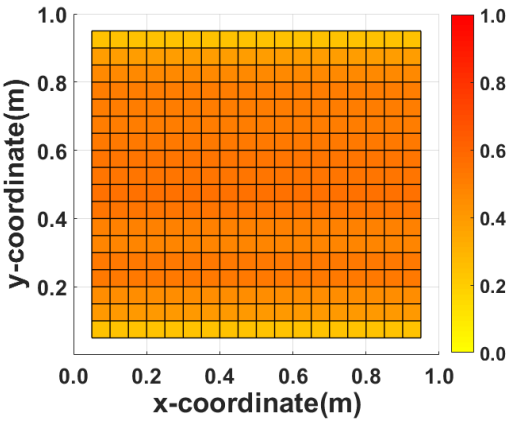

(a) [0/90/90/0]

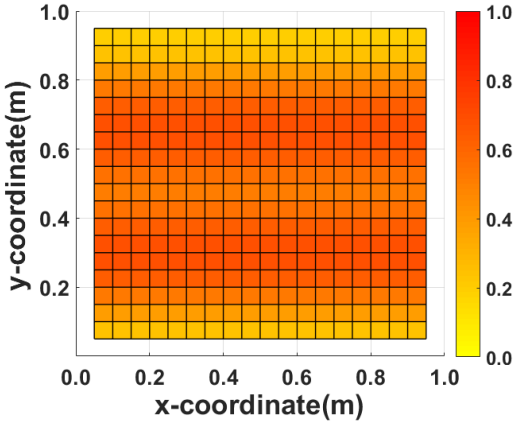

(b) [45/-45/-45/45]

Fig. 13 Induced correlation coefficients of the reconstruction of dynamic responses of composite for all measurement locations (central loading, Case II)

the local modes are not major factors in the overall behavior of laminated composites subjected to impact loads. For the global mode, the reconstructed time history data agree well with the measured data, regardless of small measurement range. The proper choice of the range of measurement influences the probability of data reconstruction. The change in reconstruction associated with different measurement locations can be ignored; the change of the fitness value is insignificant. This research addresses the applicability of the combined Micro-GA and gamma function to estimate the location of delamination and associated behavior in a composite structure.

4.3 Correlation coefficient for different fiber angles

Figs. 12 and 13 show contours of the correlation coefficients between the measured and reconstructed responses. In the figures, the red contours indicate a high correlation between the two data while the yellow contours indicate a low correlation between the two data. As expected, the reconstructed responses obtained from this research are well-correlated to the true ones except for few points near the boundaries. For the two cases, the correlation coefficients also show that the response predictions for [±45/-45]s laminate are more accurate than those for [0/90]s laminate. Additionally, there is a significant increase of coefficients at the central points in comparison to the plate edges. This is predictable because it is expected that the wave propagation speed and magnitude increase near the loading points. The accuracy of the reconstruction depends on many parameters such as ply angles, loading and measurement points, and locations of delamination.

5. Conclusions

In this research, the delamination of laminated composites under impact loads was identified from a combination of mathematical and numerical methods. The proposed approach using a modified bivariate gamma function presents excellent numerical efficiency and applicability for real structures. The stiffness reduction owing to delamination is relatively accurately transformed to damaged shapes through use of the modified bivariate gamma function. The following conclusions were made

from the parametric results obtained in this study.

• In the two-dimensional finite element formulation on the basis of the first shear deformation theory, three different types of elements were used at the boundaries of a delamination. The results using the proposed two-dimensional delamination model agree well with those reported in an existing study. This model is recommended to be used for the effective memory management and efficiency of the iterative computation.

• The combined Micro-GA and gamma function method is computationally efficient since it enables to optimize the location of damage with a small number of unknown parameters. The high sensibility of this method enables to detect the damage from only slight change in the dynamic response data associated with the delamination.

• The rate of the detection convergence is dependent on the location of the delamination and loading and measurement condition. The layup sequence of laminates also has an influence on the probability of detection. Therefore, it is required to optimize the measurement location and loading condition for the better convergence.

• The reconstructed responses induced from this research match well with the measured ones except for few points near the boundaries. It is found that there is a significant increase of the reconstruction sensibility at the central points in comparison to the plate edges. This is associated with the increase of the wave propagation speed and magnitude near the loading points.

Acknowledgments

This work was supported by the National Research Foundation of Korea (NRF) grant funded by the Korea government (MSIP) (no. 2018R1D1A1B07050080). This work is also financially supported by Ministry of Public Administration and Security as Disaster Prevention Safety Human Resource Development Project.

References

Achache H., Benzerdjeb, A., Mehidi A., Boutabout, B. and Ouinas, D. (2017), "Delamination of a composite laminated under monotonic loading", *Struct. Eng. Mech.*, **63**(5), 597-605.

Bhattacharya, M., Islam, R. and Abawajy, J. (2016), "Evolutionary optimization: A big data perspective", *J. Netw. Comput. Appl.*, **59**, 416-426.

Chandrashekhar, M. and Ganguli, R. (2016), "Damage assessment of composite plate structures with material and measurement uncertainty", *Mech. Syst. Sign. Proc.*, **75**(15), 75-93.

Gunst, R.F. and Webster, J.T. (1973), "Density functions of the bivariate chi-square distribution", *J. Stat. Comput. Simul.*, **2**, 275-288.

Hu, N., Fukunaga, H., Kameyama, M., Aramaki, Y. and Chang, F.K. (2002), "Vibration analysis of delaminated composite beams and plates using a higher-order finite element", *Int. J. Mech. Sci.*, **44**(7), 1479-1503.

Hua, N., Fukunaga, H., Kameyama, M., Aramaki, Y. and Chang, F.K. (2002), "Vibration analysis of delaminated composite beams and plates using a higher-order finite element", *Int. J. Mech. Sci.*, **44**(7), 1479-1503.

Ju, F., Lee, H.P. and Lee, K.H. (1995), "Finite element analysis of free vibration of delaminated composite plates", *Compos. Eng.*, **5**(2), 195-209.

Kassapoglou, C. (2015), *Modeling the Effect of Damage in Composite Structures*, Wiley & Sons Ltd, West Sussex, U.K.

Kim, B.H., Lee, I.K. and Cho, S.J. (2012), "Estimation of existing prestress level on bonded strand using impact-echo test", *Proceedings of the 6th European Workshop on Structural Health Monitoring*, Dresden, Germany.

Lee, S.Y. and Noh, M.H. (2014), "An advanced coupled genetic algorithm for identifying unknown moving loads on bridge decks", *Math. Probl. Eng.*, 1-11.

Lee, S.Y. and Park, T. (2009), "Free vibration of laminated composite skew plates with central cutouts", *Struct. Eng. Mech.*, **31**(5), 587-603.

Lee, S.Y. and Wooh, S.C. (2005a), "Detection of stiffness reductions in laminated composite plates from their dynamic response using the microgenetic algorithm", *Comput. Mech.*, **36**(4), 320-330.

Lee, S.Y., Park, T. and Voyiadjis, G.Z. (2008b), "Detection of stiffness reductions in concrete decks with arbitrary damage shapes using incomplete dynamic measurements", *J. Eng. Mech.*, **134**(7), 567-577.

Lee, S.Y., Rus, G. and Park, T. (2007), "Detection of stiffness degradation in laminated composite plates by filtered noisy impact testing", *Comput. Mech.*, **41**(1), 1-15.

Lee, S.Y., Rus, G. and Park, T. (2008a), "Quantitative nondestructive evaluation of thin plate structures using the complete frequency information from impact testing", *Struct. Eng. Mech.*, **28**(5), 525-548.

Lee, S.Y. and Wooh, S.C. (2005b), "Waveform-based identification of structural damage using the combined FEM and microgenetic algorithms", *J. Struct. Eng.*, **131**(9), 1464-1472.

Luca, A.D., Sharif-Khodaei, Z., Aliabadi, M.H. and Caputo, F. (2016), "Numerical simulation of the Lamb wave propagation in impacted CFRP laminate", *Proc. Eng.*, **167**, 109-115.

Mokaddem, A., Alami, M., Doumi, B. and Boutaous, A. (2014), "Prediction by a genetic algorithm of the fiber-matrix interface damage for composite material. Part 1. Study of shear damage in two composites T300/914 and PEEK/APC_2", *Strength Mater.*, **46**(4), 543-547.

Noh, M.H. and Lee, S.Y. (2013), "A bivariate Gaussian function approach for inverse cracks identification of forced-vibrating bridge decks", *Inv. Probl. Sci. Eng.*, **21**(6), 1047-1073.

Noh, M.H. and Lee, S.Y. (2014), "Dynamic instability of delaminated composite skew plates subjected to combined static and dynamic loads based on HSDT", *Compos. Part B Eng.*, **58**, 113-121.

Park, T. and Lee, S.Y. (2009), "Parametric instability of delaminated composite spherical shells subjected to in-plane pulsating forces", *Compos. Struct.*, **91**(2), 196-204.

Park, T., Noh, M.H., Lee, S.Y. and Voyiadjis, G.Z. (2009), "Identification of a distribution of stiffness reduction in reinforced concrete slab bridges subjected to moving loads", *J. Brid. Eng.*, **14**(5), 355-365.

Qi, X., Zhao, X. and Rose, J.L. (2009), "Ultrasonic guided wave simulation toolbox development for damage detection in composites", *AIP Conf. Proc.*, **1211**(1), 1095-1102.

Rus, G. and Lee, S.Y. (2016), "Optimal reconstruction of the damage distribution in bridge decks by measuring the noisy response induced by traffic loads", *KSCE J. Civil Eng.*, **19**(6), 1832-1844.

Rus, G., Lee, S.Y. and Gallego, R. (2005), "Defect identification in laminated composite structures by BEM from incomplete static data", *Int. J. Sol. Struct.*, **42**(5-6), 1743-1758.

Rus, G., Lee, S.Y., Chang, S.Y. and Wooh, S.C. (2006),

"Optimized damage detection of steel plates from noisy impact test", *Int. J. Numer. Meth. Eng.*, **68**(7), 707-727.
Sharif-Khodaei, Z., Ghajari, M. and Aliabadi, M.H. (2015), "Impact damage detection in composite plates using a self-diagnostic electro-mechanical impedance based structural health monitoring system", *J. Multisc. Mod.*, **6**(4), 1-20.
Smith, O.E., Adelfang, S.I. and Tubbs, J.D. (1982), *A Bivariate Gamma Probability Distribution with Application to Gust Modeling*, NASA Technical Memorandum, NASA-TH-82483.
Trung, V.D., Vinh, H.H., Hau, D.T., Du, D.C. and Trung, N.T. (2016), "Damage detection in laminated composite plates using modal strain energy and improved differential evolution algorithm", *Proc. Eng.*, **142**, 182-189.
Williams, W.B., Michaels, T.E. and Michaels, J.E. (2017), "Estimation and application of 2-D scattering matrices for sparse array imaging of simulated damage in composite panels", *AIP Conf. Proc.*, **1806**(1), 020014-1-020014-9.

CC